OPEN-MIDPLANE DIPOLES FOR A MUON COLLIDER*

R. Weggel#, J. Kolonko & R. Scanlan, Particle Beam Lasers, Northridge, CA
D. Cline & X. Ding, UCLA, Los Angeles, CA 90095, USA
M. Anerella, R. Gupta, H. Kirk, B. Palmer & J. Schmalzle, BNL, Upton, NY

Abstract

For a muon collider with copious decay particles in the plane of the storage ring, open-midplane dipoles (OMD) may be preferable to tungsten-shielded cosine-theta dipoles of large aperture. The OMD should have its midplane completely free of material, so as to dodge the radiation from decaying muons. Analysis funded by a Phase I SBIR suggests that a field of 10-20 T should be feasible, with homogeneity of 1x10^{-4} and energy deposition low enough for conduction cooling to 4.2 K helium. If funded, a Phase II SBIR would refine the analysis and build and test a proof-of-principle magnet.

CONCEPT, FIELD, FORCES & STRESSES

Dipole Magnet with Truly Open Midplane

For muon colliders, cos(θ) dipoles are expensive because of the large bore needed to accommodate shielding to protect the conductor from radiation from the decaying muons. Open-midplane dipole (OMD) designs [1] banish windings from the path of this radiation. The design concept proposed here—an outgrowth of R&D for an LHC luminosity upgrade [2, 3]—banishes **structure**, too, from the midplane. The windings closest to the midplane are supported via magnetic attraction from outboard windings embedded in stainless steel [Fig. 1].

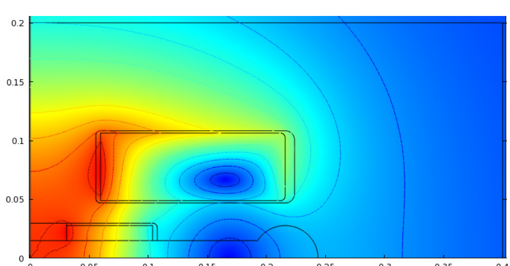

Figure 1: Cross section & field magnitude in 1st quadrant of an OMD. Half-gap = 15 mm; structural support: x_{max}= 40 cm; y_{max}= 20 cm. Muon beam is at [0, 0]. Lobed end of keyhole accommodates a radiation absorber of tungsten.

Fields & Forces: Equations & FEM Modeling

To generate designs with optimized combinations of central field B_0, field homogeneity $\Delta B/B_0$, peak-field ratio B_{max}/B_0 and conductor volume or cost, while guaranteeing that the vertical magnetic force on each inboard coil will attract it away from the midplane, analytic equations are preferable to FEM methods to compute the fields and forces. For a bar of infinite length, rectangular X-section and uniform current density J, the vertical field B_y is [4]:

$$\sum_{i=1,j=1}^{i=2,j=2} (-1)^{i+j}\, c_B\, v_j\, \ln(u_i^2 + v_j^2) + 2v_j \tan^{-1}\left(\frac{u_i}{v_j}\right),$$

where $c_B = \mu_0 J$, and u_i and v_j are shorthand for $a_i - x$; and $b_j - y$, the horizontal and vertical distances, respectively, from a bar corner $[a_i, b_j]$ to the field point $[x, y]$. B_x is of the same form, with u_i and v_j interchanged.

The vertical force F_y between two bars has sixteen terms of the form:

$$c_F\{(3v^2 - u^2)\, u\, \ln(u^2+v^2) + 2v[3u^2 \tan^{-1}\left(\frac{v}{u}\right) + v^2 \tan^{-1}\left(\frac{u}{v}\right)]\},$$

where $c_F = \mu_0 J_1 J_2/6$, and u and v are shorthand for $u_{i,m}$ and $v_{j,n}$, the horizontal and vertical distances between bar corners $[a_i, b_j]$ and $[a_m, b_n]$; i, j, m and n each run from 1 to 2. For the horizontal force F_x, interchange u and v. Field and force formulas are analytic for bars of finite length, too, and are well-behaved even for bars with faces mitred to approximate conductors that curve [5].

The OMD of Fig. 1 has a central field of 10 T at 200 A/mm^2 and a peak field ratio of only 107%. $\Delta B/B_0$ is 0.01% everywhere within the red curve of Fig 2.

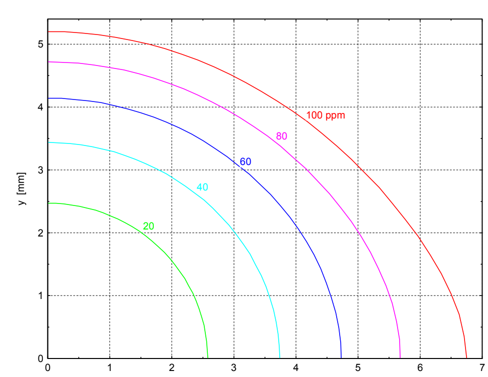

Figure 2: Contours of field-homogeneity $\Delta B/B_0$ of OMD of Fig. 1. $\Delta B/B_0$ = 1x10^{-4} at [6.7 mm, 0] & [0, 5.2 mm].

The inboard bar of conductor experiences a vertical force that is upward not only in total but on each half separately, to preclude tipping toward the midplane. The horizontal force totals 1356 kN/m. The forces on the outer bar are F_y = −3650 kN/m and F_x = 4194 kN/m.

*Supported by the U.S. DOE under Contract No. DE-AC02-98CH10886 and SBIR contract DOE grant Nos. DE-FG02-07ER84855 & DE-FG02-08ER85037

#bob_weggel@mindspring.com

Finite-element computations confirm that support structure of sufficiently great cross section can limit stresses and deformations to acceptable levels with a central field of well over 10 T, and maybe even 20 T. The von Mises stress [Fig. 3] to the right of the keyhole is benign, being compressive. The average tension in the web between the inboard and outboard bar is only ~150 MPa at 10 T; the predicted maximum deformation—not yet reduced by stress management—is less than 0.27 mm [Fig. 4]. At 20 T the tension would be ~600 MPa—acceptable for some stainless steels, especially when cold.

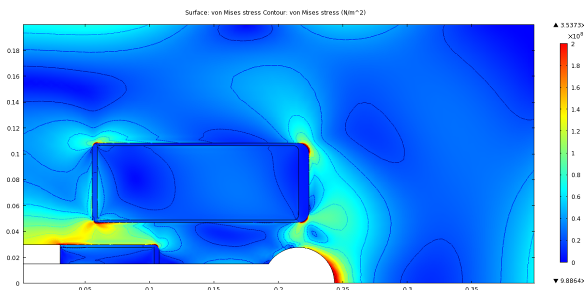

Figure 3: Contours of von Mises stress, σ_{vM}. The maximum value to the right of the keyhole is 246 MPa at 10 T; the average tension in the web is ~150 MPa.

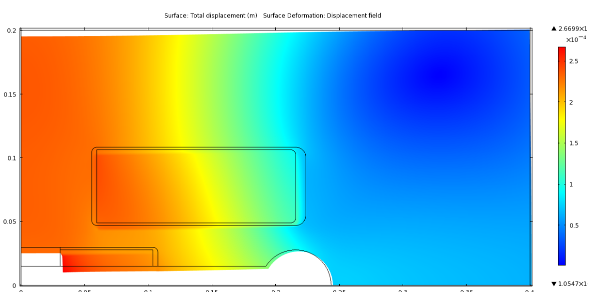

Figure 4: Predicted deformation, magnified twentyfold.

ENERGY-DEPOSITION PREDICTIONS

In a 1.5 TeV center-of-mass muon collider storage ring, muons decay to electrons at a rate of $5x10^9$/s per meter of ring. About 1/3 of the muon energy is carried by electrons, which are deflected toward the inside of the ring by the dipole magnetic field. The radiation (energetic synchrotron photons and electromagnetic showers) is ~200 W/m, mostly in the horizontal plane of the storage ring. The energy deposition must not exceed the quench tolerance of the superconducting coils. To predict the energy deposition we use the code MARS15 [3].

For our simulations we assume two counter-circulating muon beams of 750 GeV, with $2x10^{12}$ muons per bunch at a rep rate of 15 Hz. Figure 5 shows the result for a unidirectional muon beam traversing an open midplane dipole of 15 mm half gap. At the downstream end of a 6-m-long dipole the peak power density is 0.13 mW/g on the right (inward) side of the bend and 0.05 mW/g on the left side. For the outboard bar the respective peak power densities are 0.14 mW/g and 0.07 mW/g. These values are comfortably below those considered acceptable [3].

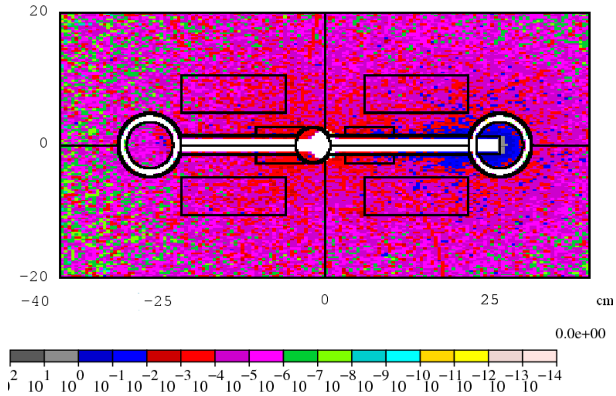

Figure 5: Energy deposition from a unidirectional muon beam at the downstream end of a 6-m-long OMD with half gap of 15 mm.

Note that the tungsten absorber has a slot in its left side, to reduce backscattering from the absorber. To eliminate backscattering completely, Kirk has suggested to obviate the right-hand absorber—the one with more backscatter radiation—by completely opening the magnet midplane on its right side, as in Fig. 6. Preliminary stress predictions suggest that such a design is indeed feasible.

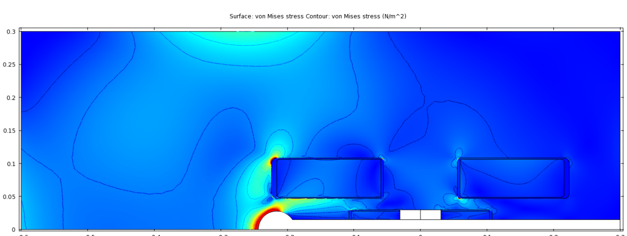

Figure 6: Von Mises stress in structure of "C" shape, w/o the right-hand absorber, to eliminate its backscattering of radiation; maximum σ_{vM} to left of keyhole = 353 MPa.

PROPOSED PROOF-OF-PRINCIPLE OMD

A major goal of a proposed Phase II SBIR is to fabricate and test a proof-of-principle (P-O-P) open-midplane dipole with the following features:

- Magnetic Lorentz forces on the inboard conductors hold them away from the midplane, so that they need no midplane support.
- The short-sample field should be ~10 T.
- The conductor is Nb_3Sn, as in a full-size 10-T OMD.
- The OMD incorporates most pertinent cold-mass components—support structure, iron yoke & keyhole to accommodate a hypothetical warm absorber.
- The OMD meets all constraints on stress, strain and deformation.

Demonstration of such a magnet will advance both muon collider feasibility and magnet technology, being the first test of a magnet with only magnetic support of inboard coils.

To be consistent with the budget of a Phase II SBIR, costs are minimized by using a bolted structure and adopting a proven LBNL Nb_3Sn double-pancake design [7]. The focus of this P-O-P magnet is to demonstrate a new design rather than to develop a new conductor technology. The design has a predicted short-sample field of ~9.7 T using Nb_3Sn strands with a critical current density of 2500 A/mm^2 at 12 T and 4.2 K with a Cu:SC ratio of 1:1; the corresponding current density in the coil is ~750 A/mm^2. Figures 7 and 8 sketch the cross section of windings and support structure.

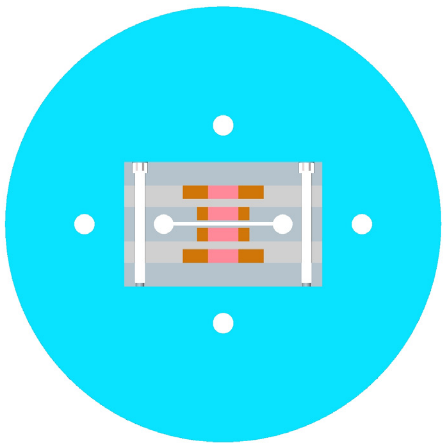

Figure 7: X-section of the proposed proof-of-principle OMD. Conductor is orange; structure is grey (stainless steel) or blue (iron). The four white circles are for tie rods to restrain end plates that resist end forces. The midplane gap would, in a muon collider, accommodate a beam pipe and, at its dumbbell ends, tungsten absorbers.

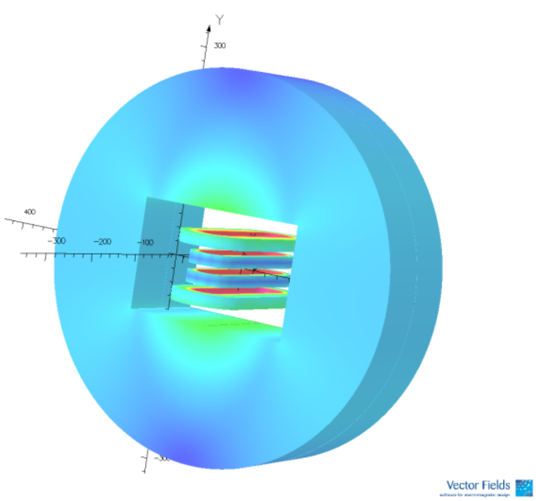

Figure 8: Racetrack coils & yoke (collar omitted for clarity). B_0 = 9.7 T at assumed short-sample current.

ANSYS calculations predict that deformations and stresses are acceptable even at a field level of 10.7 T, 10% higher than short-sample. The maximum stress predicted in the stainless steel support structure is ~400 MPa (Fig. 9), a comfortable value for stainless steel.

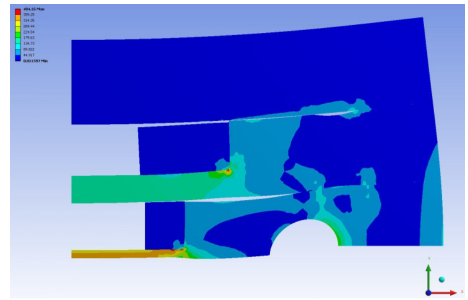

Figure 9: Von Mises stress, σ_{vM}, at B_0 = 10.7 T, which overestimates the stress by 21%; max. $\sigma_{vM} \approx$ 400 MPa.

ANSYS predicts the maximum deformation at a central field of 10 T to be only 87 μ in the structure and, more importantly, only ~ 20 μ in the coils (Fig. 10).

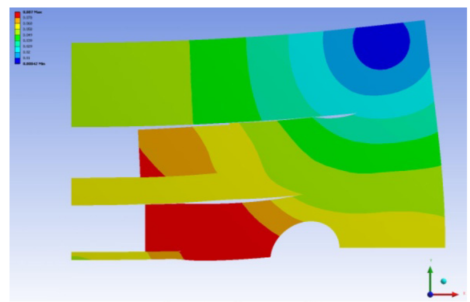

Figure 10: Total deformation δ on support structure at B_0 = 10.7 T; δ_{max}= 87 μ; coil $\delta_{max}\approx$ 20 μ.

SUMMARY

A Phase I SBIR has advanced the feasibility of open-midplane dipoles for the storage ring of a muon collider. A proposed Phase II SBIR would refine these predictions of stresses, deformations, field quality and energy deposition. Design optimizations would continue, leading to the fabrication and test, for the first time, of a proof-of-principle dipole of truly open-midplane design.

REFERENCES

[1] J. Zbasnik, et al., IEEE Trans. on Appl. Supercond., vol. 11, p. 2531 (2002).

[2] R. Gupta, et al., "Optimization of Open Midplane Dipole Design for LHC IR Upgrade," PAC'05, Knoxville, USA (2005).

[3] N.V. Mokhov, et al., "Energy Deposition Limits in a Nb_3Sn Separation Dipole in Front of the LHC High Luminosity Triplet", PAC'03, Portland, USA (2003).

[4] D.B. Montgomery, assisted by R. Weggel, *Solenoid Magnet Design*, 2nd printing, Krieger (1980).

[5] C. Weggel, in Los Alamos Accelerator Code Group, *Computer Codes for Particle Accelerator Design and Analysis: A Compendium*, 2nd edition, p. 104 (1990).

[6] N.V. Mokhov, http://www-ap.fnal.gov/MARS/.

[7] D.R. Dietderich, et al., "Correlation Between Strand Stability and Magnet Performance," ASC (2004).